J.Serb.Chem.Soc. 65(9)649-660(2000)
JSCS-2788

UDC 546.96'824".821"'-/54-88/:541.182.644
Original scientific paper

The effect of the presence of alcohol in the dispersing phase of oxide sols on the properties of RuO_2-TiO_2/Ti anodes obtained by the sol–gel procedure

V. PANIĆ[1#], A. DEKANSKI[2#], S. MILONJIĆ[3#], R. ATANASOSKI [2#*], and B. NIKOLIĆ[1#]

[1]*Faculty of Technology and Metallurgy, University of Belgrade, Karnegijeva 4, P. O. Box 3503, YU-11120 Belgrade (e-mail: bane@elab.tmf.bg.ac.yu),* [2]*ICTM - Center for Electrochemistry, Njegoševa 12, P. O. Box 815, YU-11001 Belgrade and* [3]*Vinča Institute of Nuclear Sciences, P. O. Box 522, YU-11001 Belgrade, Yugoslavia*

(Received 2 March 2000)

The effect of the addition of ethanol and 2-propanol to the dispersing phase of TiO_2 and RuO_2 sols mixture on the morphology and, consequently, on the electrochemical properties of the sol-gel obtained activated titanium anodes was investigated. The properties of the obtained anodes were compared to those obtained by the thermal decomposition of appropriate chloride salts. The morphology of the anode coatings was examined by scanning tunneling microscopy. The electrochemical behaviour was investigated by cyclic voltammetry and by polarization measurements. An accelerated stability test was used for the examination of the stability of the anodes under simultaneous oxygen and chlorine evolution reaction. A dependence of the anode stability on the type of added alcohol is indicated.

Keywords: activated titanium anodes, RuO_2 sol, TiO_2 sol, sol-gel procedure, accelerated stability test.

INTRODUCTION

Noble metal oxides, dominantly RuO_2 and IrO_2, applied onto titanium supports were initially developed for industrial use as anodes in chlor-alkali electrolysis and as oxygen-generating anodes in electrolytic plating.[1,2] Today they are known as good electrocatalyts for a number of electrochemical processes.[3–6] The preparation of such anodes involves the thermal decomposition of chloride precursors, previously dissolved in an appropriate solvent.[1,7,8] The obtained electrode coatings are known to be porous, with a large real surface area that can be enlarged by the addition of TiO_2, SnO_2 and Ta_2O_5, which primary act as stabilizing components.[2] The latest trends are focused on the investigation of the basic electrode prop-

Serbian Chemical Society active member.

* Present address: 3M Center, St. Paul, Mn 55144, USA.

erties (both morphological and electrochemical) affected either by implantation of numerous different oxides[9–13] or by different techniques of oxide preparation, among which the sol-gel procedure seems to be very promising.[14–16] The basic goal is to achieve the largest possible real surface are and to discriminate the effects of geometric factor on the electrocatalytic activity from those of surface electronic states, which can be correlated with the surface acid-base properties of the electrode.[17,18] This discrimination can be realized by point of zero charge (pzc) measurements, taking the pH value of the solution in which the oxide surface is electrically neutral as the pzc,[17,18] or by blocking the characteristic active sites with some organic molecules, which results in a decrease of the charge on the surface.[11]

As was shown in our previous work,[16] the forced hydrolysis of extremely acid solutions of $RuCl_3$ and $TiCl_3$ is a good method for the preparation of oxide sols. The obtained RuO_2 and TiO_2 sols, appropriately applied onto Ti support and calcinated, form an electrocatalytic coating with similar basic electrochemical properties to those prepared by thermal decomposition, but the sol-gel anodes last longer under the rigorous conditions of an accelerated stability test (AST)[7,8] than those thermally prepared.

The aim of this work was to study the effect of the dispersing medium composition on the size, shape and distribution of the oxide particles and, consequently, on the coating properties. Namely, modification of the sol composition changes the surface tension of the sol mixture, which causes different shape of the sol drops on the surface. This should affect the morphology of the coatings. The sol composition was modified by the addition of ethanol and 2-propanol to the dispersing medium. However, the addition of alcohols also affects the sol stability. Hence, not only was the effect of alcohol in the dispersion medium on the morphology and electrochemical properties of anodes determined but also its effect on the stability of the sol mixture. The properties of anodes prepared by deposition of such modified sol mixtures were compared with those of anodes prepared without the modification as well as with those anodes obtained by thermal decomposition.

EXPERIMENTAL

The TiO_2 and RuO_2 sols were prepared following the procedure of forced hydrolysis.[16] Titanium trichloride (Merck, 10 % $TiCl_3$ in 15 % aqueous HCl) and ruthenium trichloride (Ventron, GmbH) were used as the starting chemicals. The obtained oxide sols were then concentrated by evaporation to obtain the optimal amount of the dispersed (solid) phase. The two oxide sols were then mixed to obtain 40 % Ru : 60 % Ti as the coating composition. The mixture was divided into three parts; to one of them ethanol and to another 2-propanol was added up to an alcohol : dispersion ratio of 50 : 50.

It was observed that ethanol, as well as 2-propanol, influences the flocculation of the solid phase. The dispersed phase became visible after several days from the moment of the addition of either alcohol, although the effect in the case of 2-propanol addition was more pronounced. Such a slow rate of destabilization (aggregation) allowed the obtained mixtures to be used fot the preparation of coatings. In this work, the mixtures prepared with the alcohols were applied 12 h after mixing. However, it is to be expected that the oxide particles from the mixtures with the alcohols would be larger than those from the sol mixture prepared without the addition of the alcohols.

Titanium plates, 1.5 × 1.5 cm in size, were used as the substrate, formerly prepared for the deposition as described elsewhere.[8,16] The deposition of the sol mixtures was achieved by multilayer painting.[8,16] Each layer was calcined at 450 °C for 10 min and a final annealing was performed at 450 °C for 30 min. The amount of the coating was 2± 0.4 mg cm^{-2} (RuO_2+TiO_2) on each anode. The denotations for the anodes are:

thl – anodes obtained by thermal decomposition;[7,8]

wtr – anodes obtained by the application of the sol mixture without alcohol addition;[16]

ipl – anodes obtained by the application of the sol mixture containing 2-propanol;

etl – anodes obtained by the application of the sol mixture containing ethanol.

The working electrode (surface area: 1 cm^2) was mounted in a Teflon holder. A Pt plate served as the counter electrode and a saturated calomel electrode (SCE) as the reference. All potentials refer to the SCE.

The anodes were examined by scanning tunneling microscopy (STM) (Nanoscope III, DI, USA) at scan sizes 880× 880 nm^2 and 50 × 50 nm^2; the surface appearance was checked using both scan sizes at three different places. Cyclic voltammetry and polarization measurements were performed with a potentiostat/galvanostat (PAR model 273A) in 5 M NaCl, pH 2, at room temperature. The sweep rate was varied in the range 3 – 500 mV s^{-1}. The accelerated stability test was done galvanostatically (j = 2 A cm^{-2}) in 0.5 M NaCl, pH 2, at 33 °C.

RESULTS AND DISCUSSION

The surface appearances of the anodes are illustrated by the STM images in Fig. 1, recorded at one of the three different locations at a scan size of 880 nm ×880 nm. These images give qualitative information about the distribution of the coating ma-

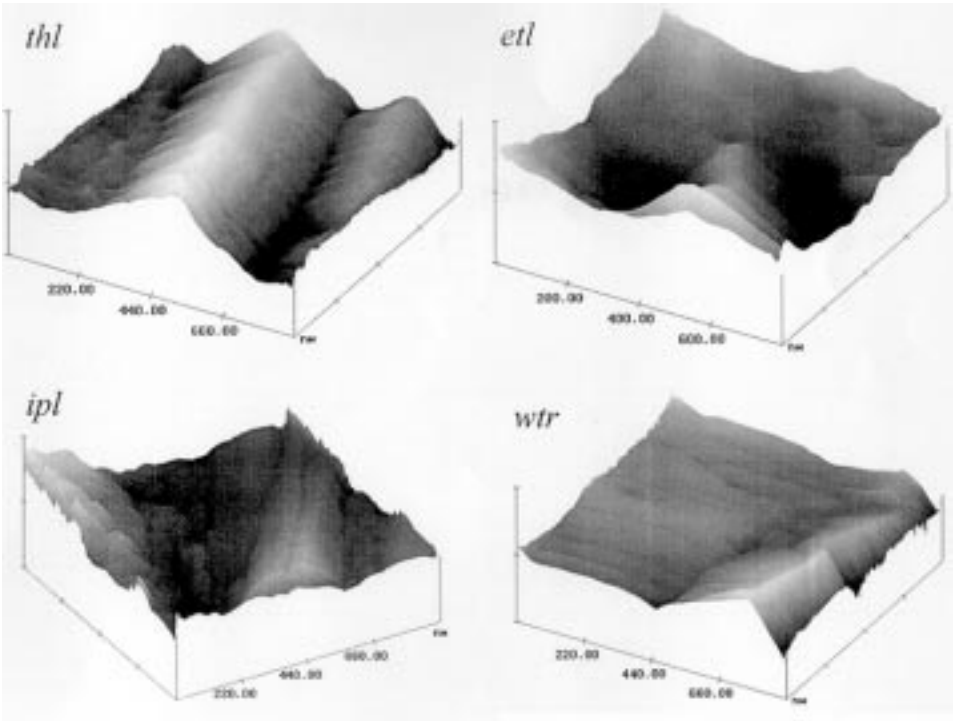

Fig. 1. STM images of the *thl*, *etl*, *ipl* and *wtr* anodes: z = 5 nm div^{-1}.

terial over a rather large area as compared to the oxide particle size, which is in the order of nanometers.[19] The most uniform distribution of the coating material was visible on the *wtr* anode, while the *thl* anode had the worst distribution. These surface differences are seen more clearly from the bar graph given in Fig. 2, which represents the average values of the three surface area differences (SAD) between the real and geometric surface areas, obtained in STM analysis. At the applied scan size of 880 nm × 880 nm, the difference between the real and geometric surface areas is about five times larger for the *thl* anode than for all the anodes obtained by the sol-gel procedure. Such a pronounced difference is probably due to the more uniform micro-distribution of the material in the sol–gel coatings than in the thermal one, which is caused by the better packing of the suitablys-haped sol–gel particles. From Fig. 2 it seems that the addition of alcohols into the sol mixture has only a small influence on the micro-distribution of the coating material.

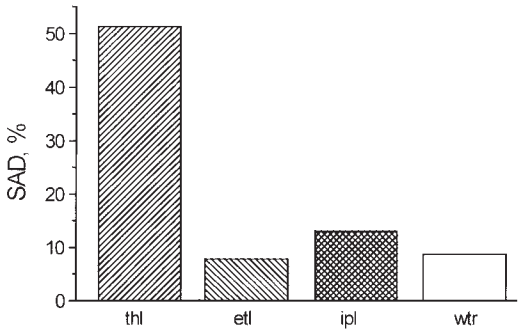

Fig. 2. The average relative difference between the real and geometric surface area (SAD) for the scanned anode surfaces shown in Fig. 1.

The STM images shown in Fig. 3 were taken at a scan size 50 nm × 50 nm, which is informative enough for the oxide particle size and shape. The ubiquitous nano-rough spots seen on the sol–gel obtained anodes were not observed on the thermal one. This observation suggests that the sol–gel obtained coatings consist of smaller grains than those thermally prepared, and consequently, they should have a larger real surface area at the nano-level. Also, the sharpest spots present on the coating surface prepared with 2-propanol addition suggest a pronounced influence of 2-propanol on the shape of the grains, which results in the *ipl* anode having the largest real surface areas when compared to other anodes. Fig. 4 represents the difference between the real and geometric surface area of the surfaces when scanned at 50 nm × 50 nm. The SAD value for the *thl* anode is the smallest, meaning the smallest real surface area or largest particles. The largest SAD value is observed for the *ipl* anode, which differs only to a small degree from that for the *wtr* anode, from which it can be concluded that there is no significant difference in particle size between these two types of coating. The small difference between the SAD values for the *wtr* and *ipl* anode is caused by the mixed influence of 2-propanol which destabilizes the sol and simultaneously changes the particle shape. The influence of ethanol on the particle shape could not be proved from Fig. 4 (nor from Fig. 3).

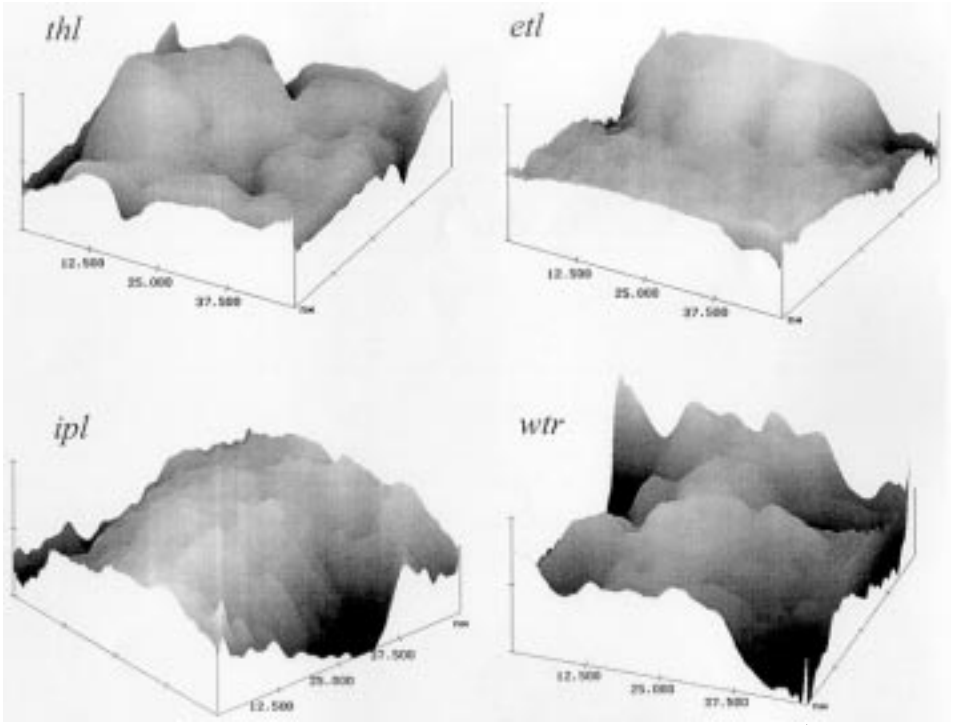

Fig. 3. STM images of the *thl*, *etl*, *ipl* and *wtr* anodes: z = 2.5 nm div^{-1}.

The cyclic voltammograms for the obtained anodes are shown in Fig. 5. They are all of similar shape, although the current values are quite different. The appearance of a broad reversible peak at about 0.5 V, attributed to the Ru^{3+}/Ru redox couple,[7,20] can be clearly seen. A several time larger anodic charge is seen for the *wtr* anode than for the *ipl* and *etl* anodes. This could be the proof[9] that the finest oxide

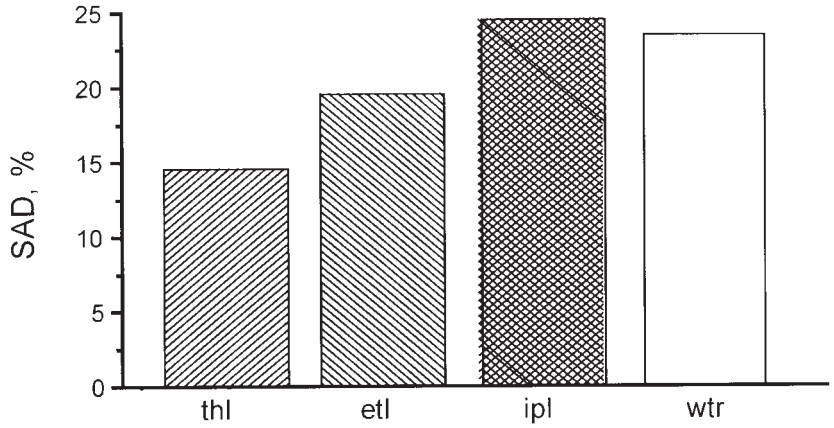

Fig. 4. The average relative difference between the real and geometric surface area (SAD) for the scanned anode surfaces shown in Fig. 3.

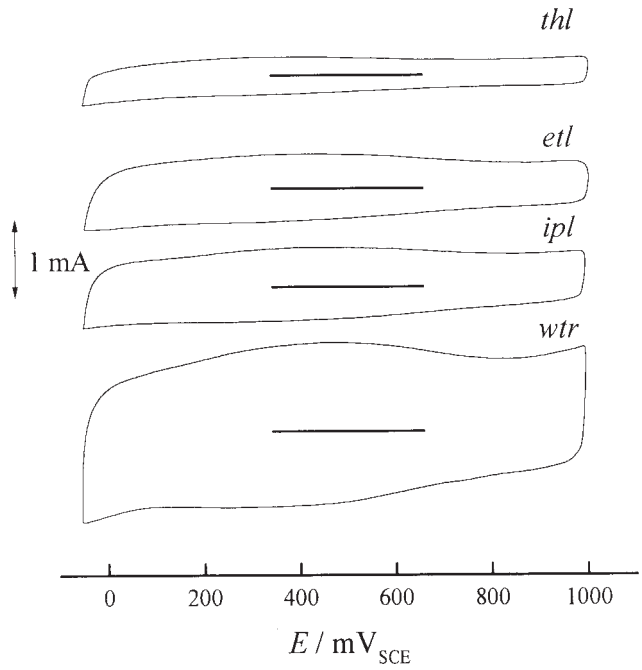

Fig. 5. Voltammetric curves for the *thl*, *etl*, *ipl* and *wtr* anodes. Electrolyte: 5 M NaCl, pH 2; sweep rate: 50 mV s^{-1}; room temperature.

particles are formed in the preparation procedure for the *wtr* anode, which was not so obvious from the STM data. To explain this, one can speculate with the fact that the anodic charge is related to the number of electrochemically active sites, which are only Ru species,[21] bearing in mind that the inactive TiO_2 component also contributes to the interpretation of the STM data. The STM data are related to the surface appearance but do not differentiate between the oxide components of the coating, although it could be expected that the added alcohols would have different effects on the RuO_2 and TiO_2 sols. Nevertheless, the general observation from Fig. 4 and Fig. 5 is that smaller grains are formed in the sol–gel procedure of coating preparation than in the thermal one.

As it was shown by Trasatti and coworkers,[10,21] the voltammetric charge of the RuO_2 coating q, C cm^{-2}, is a measure of the number of active sites onto which protons are reversibly exchanged with the solution:

$$RuO_x(OH)_y + \delta H^+ + \delta e^- \rightleftarrows RuO_{x-\delta}(OH)_{y+\delta}; \quad 0 \le \delta \ge 2 \tag{1}$$

According to this approach, the dependence of the apparent anodic charge density, calculated by integration of the anodic part of the voltammetric curve, on sweep rate v, V s^{-1}, can be interpreted by two phenomenological relations which are not directly related in an analytical sense:

$$q = q_{out} + kv^{-1/2} \tag{2}$$

and

$$1/q = 1/q_{tot} + k'v^{1/2} \quad (3)$$

assuming that:

$$q_{tot} = q_{out} + q_{in} \quad (4)$$

where q_{tot} is the charge density related to all active sites, including "hidden", less accessible ones (grain boundaries, pores and cracks), q_{in} is related to the "hidden" sites and q_{out} is related to the outer sites which are directly exposed to the electrolyte while k and k' are constants. Less accessible regions of the coating become progressively excluded as the rate of reaction (1), or sweep rate is enhanced, so from Eqs. (2) and (3) one obtains:

$$q \rightarrow q_{out} \text{ when } v \rightarrow \infty \quad (5a)$$

and

$$q \rightarrow q_{tot} \text{ when } v \rightarrow 0 \quad (5b)$$

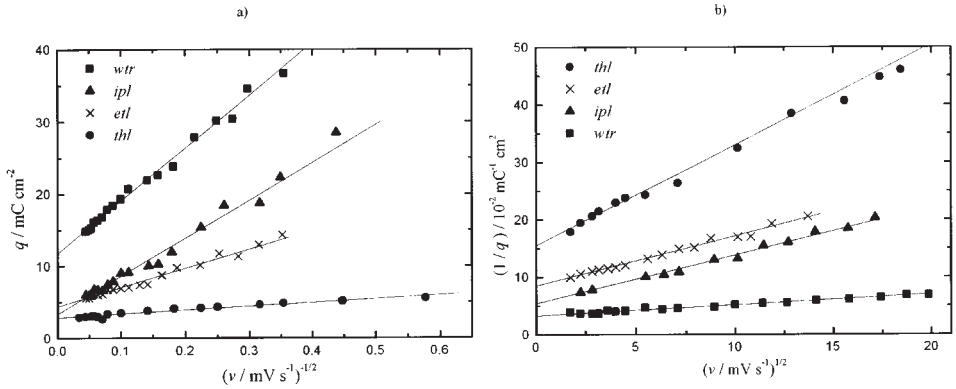

Fig. 6. a) q *vs.* $v^{-1/2}$ and b) q^{-1} *vs.* $v^{1/2}$, plots for the *thl*, *etl*, *ipl* and *wtr* anodes. The voltammetric charges were obtained by integration of the anodic part of voltammetric curve scanned in 5 M NaCl, pH 2, between 0 and 850 mV.

The characteristic plots q *vs.* $v^{-1/2}$ and $1/q$ *vs.* $v^{1/2}$ are shown in Fig. 6. The voltammetric charge is obtained by integration of the anodic part of the voltammetric curve within the potential range 0 – 850 mV. The numeric values of the characteristic charges obtained by extrapolation of the linear functions from Fig. 6 are given in Table I. The values for q_{tot} lead to the same conclusion about the difference in grain size as was reached from STM analysis and Fig. 5 – the highest value is obtained for the *wtr* anode and the smallest for the *thl* anode.

The values for q_{out} can be related to the STM data from Fig. 4. Higher values for q_{out} are observed for sol–gel obtained anodes than for the thermally obtained one, which agrees with the STM observation, although these values for the sol–gel

obtained anodes do not change as observed in the bar graph from Fig. 4. This behaviour could be caused by different states of the TiO_2 matrix, which is affected by the presence of ethanol and 2-propanol in the sol mixture, as has already been discussed.

TABLE I. Characteristic charge densities obtained from the plots in Fig. 6.

Electrode	q_{out} / mC cm^{-2}	q_{tot} / mC cm^{-2}	q_{in} / mC cm^{-2}
wtr	11.76	30.38	18.62
thl	2.86	6.43	3.57
etl	4.39	11.74	7.35
ipl	3.37	18.33	14.96

The q_{in} values are a measure of the inner surface area – bulk cracks and pores between grains. The large q_{in} values suggest either the presence of pores beween large grains or the presence of narrow bulk cracks in the coatings consisting of small grains. Since the *wtr* anode consisted of the smallest grains, the obtained highest q_{in} value means the existance of bulk cracks. Also, it can be concluded that the bulk cracks are narrow, as the q_{in} value is greater than the q_{out} value. The larger q_{in} values as compared to q_{out} of the *thl* and *etl* anodes also confirms the presence of narrow bulk cracks. However, the grains are larger than in the case of the *wtr* anode, since their q_{in} values are considerably smaller. The existance of pores between grains of the *wtr*, *thl* and *etl* anodes cannot be confirmed by values of q_{in} and q_{out}. Actually, if pores exist between grains, the q_{in} and q_{out} values should not be comparable.

The surprisingly large q_{in} value for the *ipl* anode, which is several times larger than the q_{out} value, is an indication for the existance of pores between the grains. The particles of the *ipl* anode are large and have a less regular shape, which leaves

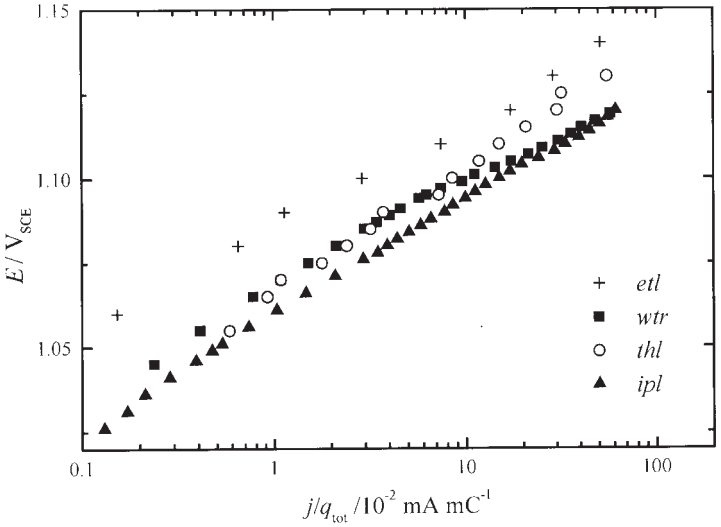

Fig. 7. The normalized Tafel plots for the *etl*, *wtr*, *thl* and *ipl* anodes. Electrolyte: 5 M NaCl, pH 2; room temperature.

wide spaces between the grains. Also, the presence of narrow bulk cracks of comparable dimensions as in the cases of the *wtr*, *thl* and *etl* anodes is to be expected.

The normalized Tafel plots are shown in Fig. 7. To discriminate the influence of the geometric factor on the current densities values, the apparent values were divided by q_{tot}.[2,19] The Tafel slopes are in the range of 30–40 mV, which are typical values of Tafel slopes for the chlorine evolution reaction on the $RuO_2 - TiO_2$ type of anodes.[22] The similarity in the activity of the *wtr* and *thl* anodes is in agreement with the observation from a previous work.[16] At this moment, it is difficult to make any further comments about the observed differences in activity between the anodes obtained with and without alcohol addition, but it could be said that this is probably due to added alcohol causing the active sites to be in different states. It is known that alcohols cause hydrogen insertion into RuO_2 resulting in a change in the oxide state.[23] Also, similar activity effects were observed in the case of RuO_2 coatings obtained from mixtures with rare earth oxides.[11–13]

The AST data, shown in Fig. 8, indicate that the *wtr* anode is the most stable under conditons of simultaneous oxygen and chlorine evolution, which take place during AST.[7,8] The *etl* and *thl* anodes have similar lifetimes, but the *ipl* anode is rather unstable.

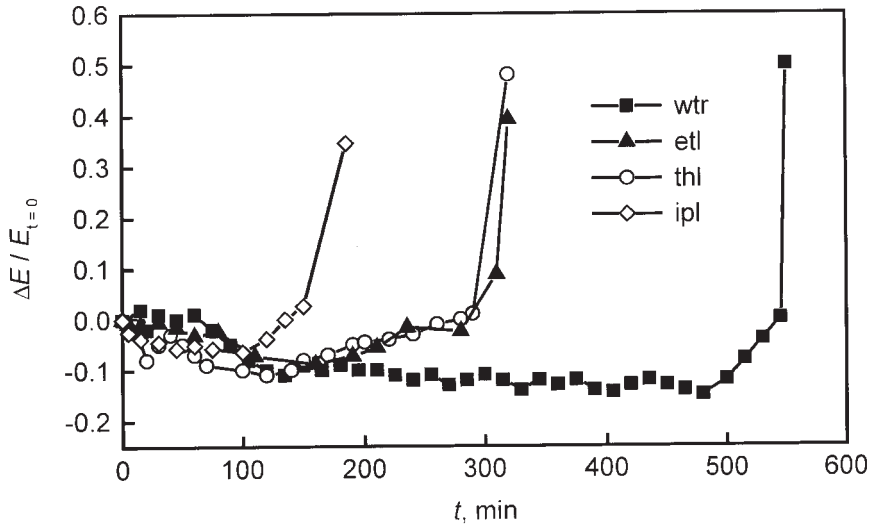

Fig. 8. The time depencence of the relative change of the electrode potential as a result of the accelerated corrosion test. Electrolyte: 0.5 M NaCl, pH 2; temperature 33 °C; $j = 2$ A cm^{-2}. . $\Delta E = E_t - E_{t=0}$. E_t – electrode potential at time t, $E_{t=0}$ – electrode potential at $t = 0$.

According to the literature,[7,8] there are two main causes for the loss of electrocatalytic activity or anode disordering. One is the selective dissolution of the electrochemically active Ru species and the other is the simultaneous formation of an insulating TiO_2 layer at the coating/Ti interface during long-term electrolysis. Which of the two dominates depends on the morphology of the coating. The smaller

grains and, consequently, the greater real surface areas of the sol–gel anodes affect the dissolution rate of the active Ru species, so that the real current density of Ru dissolution is smaller in the case of the sol–gel anodes than in the case of the thermal one. Also, the electrolysis current appears to be better distributed due to the narrow particle size distribution, which is provided by the sol–gel procedure of oxide synthesis.[24] Although high porosity significantly contributes to the surface area enlargement, at the same time it enables penetration of the electrolyte into the coating where, due to diffusion limitation of the chlorine evolution reaction, the oxygen evolution reaction dominates. The evolved oxygen diffuses towards the substate/coating interface causing the growth of an insulating TiO_2 interlayer.[7] The optimal value of the porosity provides a high real surface area, but with slow electrolyte penetration. This is achieved with the *wtr* anode. In the case of the *ipl* anode, the porosity is so high that electrolyte penetration is practically unhindered. As a result of this, the ohmic drop, caused by increased TiO_2 at the interface, becomes significant immediately after the beginning of AST on this type of anode. An increase of the electrode potential and loss of activity is the consequence.

The comparable rates of both processes responsible for the loss of activity were established on the *thl* and *etl* anodes, since they have smaller real surface areas than the *wtr* anode. The dissolution of Ru from these anodes is accelerated as compared to the *wtr* anode, but the porosities should have similar values. As a consequence, the *thl* and *etl* anodes have practically the same lifetimes, which are considerably shorter than for the *wtr* anode.

Considering the experimental results and comments, a kind of mechanism for the loss of electrocatalytic activity can be suggested for each anode. A qualitative overview is given in Table II. The check mark is used to indicate the significance of the appropriate process. The number of check marks indicates the rate of the process in the proposed mechanism. Also, the number of check marks per anode inidicates its relative stability, as was observed in Fig. 8.

TABLE II. The proposed dominating processes in the mechanism for the loss of the anode electrocatalytic activity

Electrode	Electrochemical dissolution of the active Ru species	Growth of an insulating TiO_2 layer at the interface
wtr	✓	to be neglected
thl	✓✓	✓
etl	✓✓	✓
ipl	✓✓	✓✓✓✓

These results of the accelerated stability test also indicate the dependence of the anode stability on the type of alcohol added to the dispersing phase of the oxide sols. According to Fig. 8, and to some more recent results which involved investigation of the influence of methanol addition,[25] it appears that an increase of the number of C atoms in the alcohol molecule decreases the anode stability. The lifetime of the anode obtained with methanol addition lay between that of the *etl* anode and *wtr*

anode. The influence of the number of C atoms could be connected to the different influence of the alcohol molecule on the aggregation of the oxide solid phase in the colloidal dispersion. As a cosequence, the oxide sols, into which different alcohols were added, have a solid phase consisting of oxide particles of different sizes. This interpretation requires more detailed investigation and these experiments are presently in progress.

CONCLUSIONS

The addition of the alcohols, ethanol or 2-propanol, into the dispersing phase of TiO_2 and RuO_2 sols causes a different growth of the oxide particles. In the case of 2-propanol addition, the oxide particles grow faster. At the same time, the application of such colloidal dispersions onto a Ti substrate improves the wetting of the surface and, consequently, allows for a more uniform distribution of the coating material. The sol–gel coatings, without and with the addition of ethanol or 2-propanol into the sol dispersing phase, consisted of smaller grains than that prepared by thermal decomposition. The sol–gel coatings have larger real surface areas. The presence of the pores between the grains were detected only in the coatings obtained with 2-propanol addition, which causes the shortest lifetime of this anode. The procedure of the coating preparation (thermal or sol–gel) does not influence the electrocatalytic activity of the anode for chlorine evolution, while the addition of alcohols in the case of the sol–gel coating preparation does. The stability of the anodes obtained by addition of alcohols seems to depend on a number of C atoms in the alcohol molecule.

Acknowledgments: The financial support of the Ministry of Science and Techology of the Republic of Serbia is gratefully acknowledged.

И З В О Д

УТИЦАЈ ПРИСУСТВА АЛКОХОЛА У ДИСПЕРЗНОЈ СРЕДИНИ ОКСИДНИХ СОЛОВА НА ОСОБИНЕ RuO_2–TiO_2/Ti АНОДА ДОБИЈЕНИХ СОЛ–ГЕЛ ПОСТУПКОМ

В. ПАНИЋ,[1] А. ДЕКАНСКИ,[2] С. МИЛОЊИЋ,[3] Р. АТАНАСОСКИ[2] и Б. НИКОЛИЋ[1]

[1]*Технолошко-металуршки факултет, Универзитет у Београду, Карнегијева 4, п. пр. 3503, 11120 Београд (е-пошта: bane@elab.tmf.bg.ac.yu),* [2]*ИХТМ - Центар за електрохемију, Његошева 12, п. пр. 815, Београд и* [3]*Институт за нуклеарне науке "Винча", п. пр. 522, 11001 Београд*

У раду је испитиван утицај додавања етанола односно изо-пропанола у дисперзну средину смеше солова TiO_2 и RuO_2 на морфологију и електрохемијске особине активираних титанских анода добијених сол–гел поступком. Особине овако добијених анода су поређене како међусобно тако и са особинама анода добијених термичким поступком из хлорида рутенијума и титана. Морфологија анодних превлака испитивана је скенирајућом тунелском микроскопијом, а електрохемијско понашање цикличном волтаметријом и поларизационим мерењима. Стабилност анода у паралелним реакцијама издвајања кисеоника и хлора испитивана је убрзаним тестом стабилности. Уочено је да морфологија, електрокаталитичка ативност и стабилност добијених анода зависи од врсте додатог алкохола.

(Примљено 2. марта 2000)

REFERENCES

1. S. Trasatti, W. O. Grady, in *Advances in Electrochemistry and Electrochemical Engineering*, Vol. 12, H. Gerisher and C. W. Tobias Eds., Wiley, New York, 1981, p. 177
2. S. Trasatti, *Electrochim. Acta* **36** (1991) 225
3. N. Spãtaru, J.-G. Le Helloco, R. Durand, *J. Appl. Electrochem.* **26** (1996) 317
4. C.-C. Chang, T.-C. Wen, *J. Appl. Electrochem.* **27** (1997) 355
5. S.-M. Lin, T.-C.Wen, *J. Appl. Elekctrochem.* **25** (1995) 73
6. E. O'Sullivan, J. White, *J. Electrochem. Soc.* **136** (1989) 2576
7. V. M. Jovanović, A. Dekanski, P. Despotov, B. Nikolić, R. T. Atanasoski, *J. Electroanal. Chem.* **339** (1992) 147
8. A. Dekanski, V. M. Jovanović, P. Despotov, B. Nikolić, R. Atanasoski, *J. Serb. Chem. Soc.* **56** (1991) 167
9. L. A. De Faria, J. F. C. Boots, S. Trasatti, *Electrochim. Acta* **42** (1997) 3525
10. O. R. Camara, S. Trasatti, *Electrochim. Acta* **41** (1996) 419
11. Y. Murakami, T. Kondo, X.-G. Zhang, Y. Takasu, *Denki Kagaku* **65** (1997) 997
12. Y. Murakami, T. Kondo, Y. Shimoda, H. Kaji, K. Yahikozawa, Y. Takasu, *J. Alloys Comp.* **239** (1996) 111
13. Y. Takasu, T. Arikawa, K. Yanase, X.-G. Zhang, Y. Murakami, *J. Alloys Comp.* **261** (1997) 172
14. M. Guglielmi, P. Colombo, V. Rigoto, G. Battaglin, A. Boscolo-Boscoletto, A. De Battisti, *J. Electrochem. Soc.* **139** (1992) 1655
15. K. Komeyama, S. Shohji, S. Onoue, K. Hishimora, K. Yahikozawa, Y. Takasu*, J. Electrochem. Soc.* **140** (1993) 1034
16. V. Panić, A. Dekanski, S. Milonjić, R. Atanasoski, B. Nikolić, *Colloids Surfaces A* **157** (1999) 259
17. L. A. De Faria, S. Trasatti, *J. Elekctroanal. Chem.* **340** (1992) 145
18. S. Ardizzone, S. Trasatti, *Adv. Colloid Interface Sci.* **64** (1996) 173
19. F. I. Mattos-Costa, P. de Lima-Neto, S. A. S. Machado, L. A. Avaca, *Electrochim. Acta* **44** (1998) 1515
20. D. Galizzioli, F. Tantardini, S. Trasatti, *J. Appl. Electrochim.* **4** (1974) 57
21. S. Ardizzone, G. Fregonara, S. Trasatti, *Electrochim. Acta* **35** (1990) 263
22. L. I. Krishtalik, *Electrochim. Acta* **26** (1981) 329
23. T. R. Jow, J. P. Zheng, *J. Electrochem. Soc.* **145** (1998) 49
24. E. Matijević, M. Budnik, L. Meites, *J. Colloid Interface Sci.* **61** (1977) 352
25. V. Panić, A. Dekanski, S. Milonjić, R. Atanasoski, B. Nikolić, *2nd Conference of the Chemical Societies of South-East European Countries,* Halkidiki, Greece, 2000, Book of Abstracts, Vol. II, p. 76.